Magnetohydrodynamic stability and evolution of magnetars

Peter Rau

Institute for Nuclear Theory, University of Washington

Theoretical Physics Colloquium at Arizona State University,
March 29, 2023

Introduction: Magnetars

- Class of neutron star for which the magnetic field is the dominant energy source
- Energetic electromagnetic outbursts (soft gamma repeaters, giant flares), persistent X-ray pulsations at periods 1–12 s (AXPs)
- Source of (at least some) fast radio bursts (FRBs) [CHIME/FRB Collaboration 2020]

Image Credit: ESA/ATG Medialab

- 30 known magnetars to date [McGill Online Magnetar Catalog], compared to ∼3,000 radio pulsars [ATNF Pulsar Database]
- Surface fields $B \sim 10^{14} - 10^{15}$ G
- Stronger internal fields $\gtrsim 10$–100 times the surface field strength. Such strong fields may also be required to power magnetar-type emission from magnetars with weak surface fields
- Internal B cannot globally exceed $\sim 10^{18}$ G without destroying the star

The magnetar model

Paczyński (1992), Duncan and Thompson (1992), Thompson and Duncan (1995, 1996):

1. Dynamo in the protoneutron star phase enhances B to 10^{15} G
2. MHD instability launches Alfvén waves into magnetosphere, depositing energy which is transferred through turbulence into a magnetically-trapped electron-positron pair plasma "fireball"
3. Part of fireball escapes as a giant flare. Repeated excitation of Alfvén waves by further instabilities (crustquakes?) excites gamma ray bursts from fireball (SGRs)
4. Soft thermal X-rays ($E \sim 10$ keV) emitted from surface, some of which are Compton scattering by pair plasma in magnetosphere to ~ 100 keV [Beloborodov 2013]

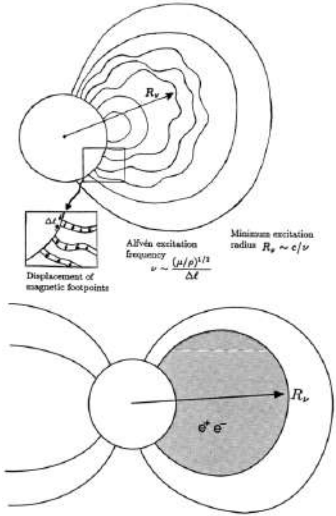

[Thompson and Duncan, MNRAS **275**, 255 (1995)]

- Confirmed by observation of X-ray pulsations from an SGR [Kouveliotou et al. 1998] and of SGRs originating from known AXPs [Gavriil et al. 2002]
- Different set of emission mechanisms for FRBs: antenna curvature radiation, synchrotron maser emission, flare-initiated magnetic reconnection, ...
- Specific emission mechanisms and what triggers them still a very active area of research

Magnetohydrodynamic (MHD) stability in stars

- Internal field structure of stars is difficult to probe, but since fields are stable, this restricts allowed forms and strengths
- E.g., Purely poloidal or toroidal fields are unstable to sausage/kink instabilities where field vanishes
- Toroidal field can be stabilized by a much weaker poloidal field [Braithwaite 2009; Akgün et al. 2013]: for neutron stars, this ratio can be $B_{\text{tor}}/B_{\text{pol}} \sim 200$

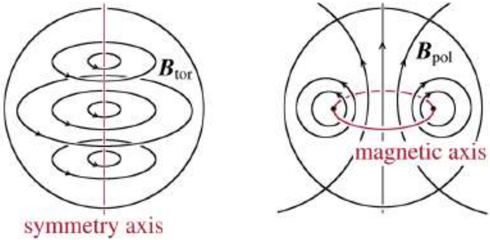

[Herbrik and Kokkotas, MNRAS **466**, 1330 (2017)]

- Stable stratification i.e., a non-barotropic equation of state (EOS) $P = P(\rho, \{X\})$, likely required for all long-term stable fields [Mitchell et al. 2015]
- A non-barotropic EOS allows for more complicated magnetic field configurations: equation of magnetohydrostatic balance is

$$\frac{\boldsymbol{\nabla} P \times \boldsymbol{\nabla} \rho}{\rho^2} = \boldsymbol{\nabla} \times \left(\frac{\boldsymbol{J}_e \times \boldsymbol{B}}{\rho c} \right),$$

  with left-hand side vanishing in barotropic limit
- Most calculations make the reasonable $B = H$ assumption (no magnetization)

Effect of strong fields: Landau quantization

- Magnetar fields exceed the electron quantum critical field $m_e^2/e = 4.4 \times 10^{13}$ G: quantum mechanical effects relevant
- Charged fermions undergo *Landau quantization* of their orbital motion perpendicular to magnetic field; most significant for electrons (quantum critical field much stronger for muons, protons)
- Landau quantization changes thermodynamic and transport properties

- E.g., energy density of an ultrarelativistic Fermi gas of electrons at $T = 0$

$$u(\mu_e, B = 0) = \frac{\mu_e^4}{4\pi^2} \to u(\mu_e, B) = \frac{eB\mu_e}{2\pi^2} \sum_{n=0}^{n_{\text{max}}} \sqrt{\mu_e^2 - 2eBn}$$

$n_{\text{max}} = \lfloor (\mu_e^2 - m_e^2)/2eB \rfloor$

- $n_{\text{max}} = 0 \to$ all electrons in a single Landau level ("strongly quantized")
- $n_{\text{max}} \gg 0 \to$ "weakly quantized", Landau quantization becomes less important
- Increased temperature smears out Landau levels; when energy difference between neighboring Landau levels $\Delta E = \sqrt{\mu_e^2 + m_e^2 + 2eB(n_{\text{max}} + 1)} - \sqrt{\mu_e^2 + m_e^2 + 2eBn_{\text{max}}} \approx T$, quantum effects start to become unimportant

- Equation of state is modified only slightly by these effects until $B \gtrsim 10^{18}$ G [Broderick, Prakash and Lattimer 2000]
- Thermal and electrical conductivities undergo Shubnikov–de Haas (SdH) oscillations; thermodynamic properties undergo de Haas–van Alphen (dHvA) oscillations

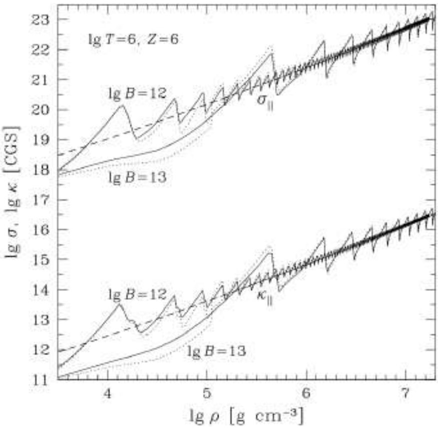

[Potekhin, A&A **351**, 787 (1999)]

E.g., dHvA oscillations in $\eta = \left.\frac{\partial H}{\partial B}\right|_{n_e} = 1 - 4\pi\chi_n(B, n_e)$;
χ_n =*differential magnetic susceptibility*. Highlighted regions:
$\eta < 0$, thermodynamically unstable

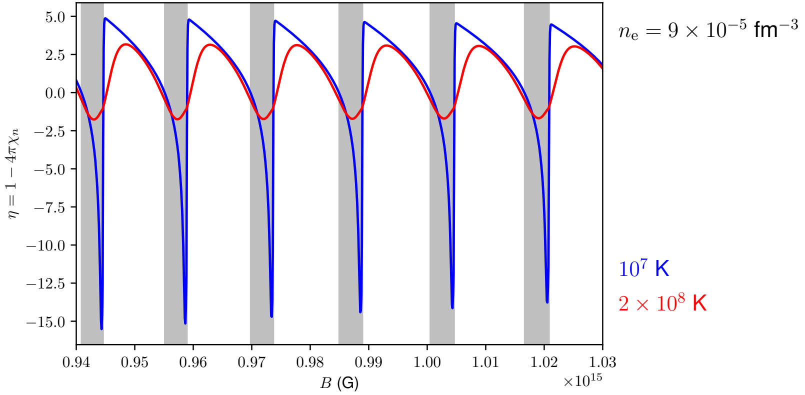

Main questions

- $B \neq H$ now, but is this difference of macroscopic significance?
- Do the quantum mechanical effects at magnetar-strength B affect MHD stability? If there are associated instabilities, could they have observable implications for magnetars?
- How important are the Landau quantization effects on thermodynamic and transport properties to magnetar magnetic field and thermal evolution?

Paper I

Magnetohydrodynamic stability of magnetars in the ultrastrong field regime I: The core – PR and I. Wasserman, MNRAS 509, 1854 (2021). arXiv:2104.08563

MHD stability analysis

- *Canonical energy* approach [Bernstein et al. 1958]: write down conserved energy E_c for a perturbed fluid configuration
- E_c depends on background fluid configuration (EOS, $\boldsymbol{B}$) and the Lagrangian displacement field $\boldsymbol{\xi} = \boldsymbol{\xi}(\boldsymbol{x}, t)$ of the perturbation
- Conservation of $E_c[\boldsymbol{\xi}] \to$ unstable modes must have $E_c[\boldsymbol{\xi}] = 0$ [Friedman and Schutz 1978]. Hence unstable modes have potential energy < 0

Local stability

- Need $\boldsymbol{\xi}$ computed using linearized Euler equation for given background fluid model to compute E_c
- Instead, look at *local* stability: define local potential energy density $\mathcal{E}_c[\boldsymbol{\xi}]$

$$E_c[\boldsymbol{\xi}] = \int_V \mathcal{E}_c[\boldsymbol{\xi}] d^3x + \text{kinetic energy}$$

  For $E_c = 0$, require $\mathcal{E}_c < 0$ in at least some regions of star
- Key Point: for $B \neq H$ MHD, $\mathcal{E}_c$ depends on second-order partial derivatives of internal energy density $u(B, \rho)$

Local stability case 1: $\boldsymbol{k} \perp \boldsymbol{B}$ perturbations

- Two criteria for $\mathcal{E}_c > 0$: stable to magnetic buoyancy (true) and magnetosonically stable

$$V^2 \equiv c_s^2 + \frac{B^2}{4\pi\rho}\eta - 2B\mathcal{M}_\rho > 0,$$

where $\eta \equiv 4\pi \left.\frac{\partial^2 u}{\partial B^2}\right|_\rho = 1 - 4\pi\chi_\rho$, $\mathcal{M}_\rho \equiv -\frac{\partial^2 u}{\partial\rho\partial B}$.

- Sound speed c_s, Alfvén velocity $v_A = \sqrt{BH/(4\pi\rho)} \approx B/\sqrt{4\pi\rho}$ stabilize fluid $\rightarrow$ No instability for $\mathbf{k} \perp \mathbf{B}$ perturbations

Local stability case 2: $\boldsymbol{k} \parallel \boldsymbol{B}$ perturbations allowed

- Four criteria for $\mathcal{E}_c > 0$, two related to magnetic buoyancy (subdominant)
- Dominant term in stability criterion is

$$K_1 \equiv \frac{B^2}{4\pi\rho}\eta - \frac{B^2\mathcal{M}_\rho^2}{c_s^2} > 0$$

- C.f. V^2, no sound speed to stabilize $\rightarrow$ instability possible if $\frac{B^2\mathcal{M}_\rho^2}{c_s^2} > \frac{B^2}{4\pi\rho}\eta$ (no) or $\eta < 0$ (yes, but *thermodynamically* unstable)

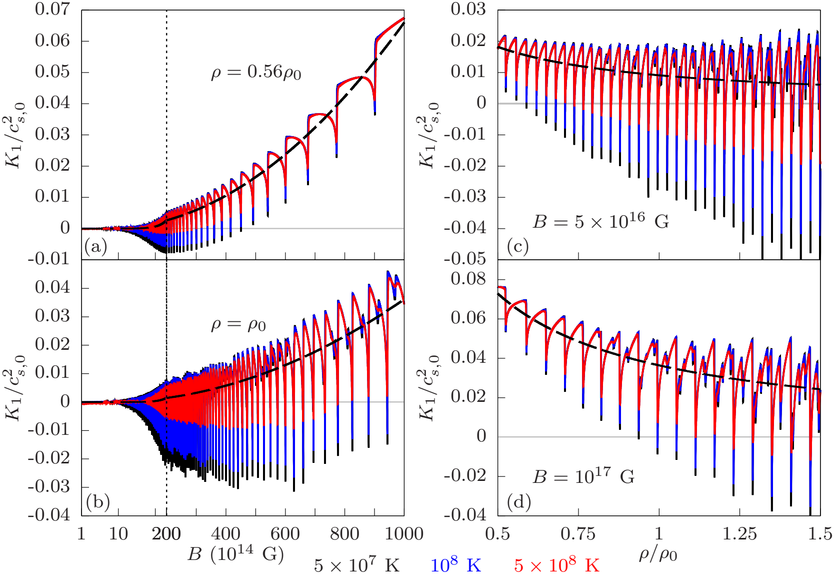

$\rho = 0.56\rho_0$
$\rho = \rho_0$
$B = 5 \times 10^{16}$ G
$B = 10^{17}$ G
(a)
(b)
(c)
(d)
$K_1/c_{s,0}^2$
$B\ (10^{14}\ \mathrm{G})$
ρ/ρ_0
5×10^7 K
10^8 K
5×10^8 K

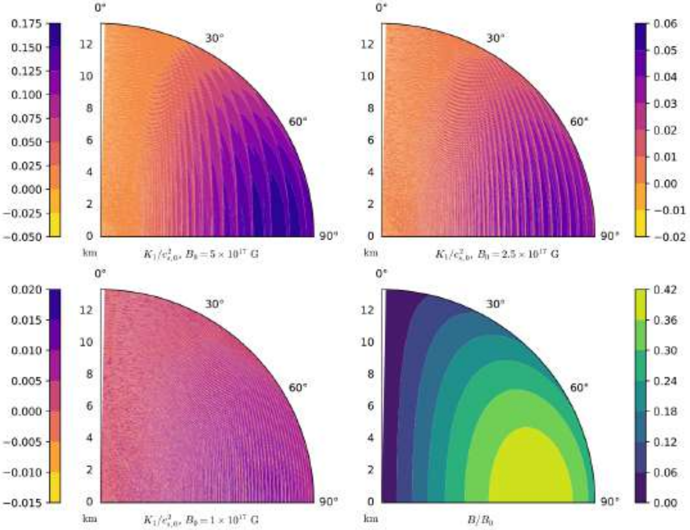

$$B = B_0 \left(\frac{\rho}{\rho_c}\right)\left(\frac{r\sin\theta}{R_\star}\right),\ T = 5\times 10^7\ \text{K}$$

Instability growth times

- These modes have a dispersion relation $\omega^2 = K_1 k_\parallel^2$, hence growth times

$$\tau \sim 2 \times 10^{-3} \left(\frac{c}{\sqrt{1000|K_1|}} \right) \left(\frac{R_\star^{-1}}{k_\parallel} \right) \text{ s}.$$

- Kinematic viscosity required to dissipate these instabilities is $\nu \sim 1/(k^2 \tau)$

$$\nu \sim 2 \times 10^{15} \left(\frac{\sqrt{1000|K_1|}}{c} \right) \left(\frac{R_\star^{-1}}{k} \right) \left(\frac{k_\parallel}{k} \right) \text{ cm}^2 \text{ s}^{-1},$$

i.e., far larger than those typical in neutron star cores $\nu \sim 10^6$–10^7 cm^2 s^{-1}

Core stability summary

- E_c is made positive by $c_s^2|\boldsymbol{\nabla}\cdot\boldsymbol{\xi}|^2 \rightarrow$ only incompressible perturbations could be unstable
- Likely result of core instability: formation of magnetic domains [Blandford and Hernquist 1982, Suh and Mathews 2010], could be destabilized later as field evolves. Rearrangement of magnetic flux to stabilize fluid on small scales- likely not relevant macroscopically

Paper II

Magnetohydrodynamic stability of magnetars in the ultrastrong field regime II: The crust – PR and I. Wasserman, MNRAS 520, 1173 (2023). arXiv:2210.05774

In the crust

- $\boldsymbol{J}_e$ is due to electrons moving with respect to a (usually) stationary nuclear lattice
- Ohm's Law becomes [Goldreich and Reisenegger 1992]

$$\boldsymbol{E} = \underbrace{-\frac{1}{c}\boldsymbol{v} \times \boldsymbol{B}}_{\text{ideal MHD}} + \underbrace{\frac{1}{\sigma}\boldsymbol{J}_e}_{\text{Ohmic diss.}} + \underbrace{\frac{1}{n_e e c}\boldsymbol{J}_e \times \boldsymbol{B}}_{\text{Hall effect}}$$

where $\boldsymbol{v} =$ mean lattice velocity ~ 0, $\boldsymbol{J}_e = \frac{c}{4\pi}\boldsymbol{\nabla} \times \boldsymbol{H}$.

Hall MHD

- Ideal MHD in the core $\rightarrow$ Hall MHD in the crust: MHD is governed by induction equation. Dissipative timescale $\gg$ Hall timescale for magnetar-strength B, hence

$$\frac{\partial \boldsymbol{B}}{\partial t} = \frac{c}{4\pi e}\boldsymbol{\nabla} \times \left[\frac{1}{n_e}\boldsymbol{B} \times (\boldsymbol{\nabla} \times \boldsymbol{H})\right]$$

- Magnetic equilibria are *not* determined by force balance equation (i.e., the Euler equation) $\rightarrow$ no conserved canonical energy [Lyutikov 2013]
- Must use perturbative analysis or numerical simulations to determine stability

Hall MHD perturbative mode analysis

- Hall ("whistler") modes: circularly-polarized, low-frequency MHD modes $\omega_{\mathsf{H}} \propto k^2 B \cos\theta_B$
- Coupling of electron motion and nuclear lattice through Lorentz force ($\boldsymbol{v} \neq 0$) [Cumming, Arras and Zweibel 2004] introduces elastic shear modes into spectrum
- With quantizing fields and elasticity, the Hall modes have dispersion

$$\omega^2 \approx \frac{\omega_{\mathsf{H}}^2 (1 - 4\pi\chi_n \sin^2\theta_B)}{(1 + \omega_{\mathsf{A}}^2/\omega_s^2)(1 - \omega_n^2/\omega_s^2)}.$$

$\omega_{\mathsf{A}} \propto kB\cos\theta_B =$ Alfvén frequency, $\omega_s =$ shear wave frequency, $\omega_n^2 \propto (\partial^2 u/\partial B \partial n_{\mathsf{e}}) \cos\theta_B$, $\theta_B = \boldsymbol{k}\angle\boldsymbol{B}$

Strong-field Hall MHD instability

- Unstable if $1 - 4\pi\chi_n \sin^2\theta_B < 0$, growth time of

$$\tau_{\mathsf{inst}} = 5 \times 10^3 |\mathsf{sec}\theta_B| \left(\frac{10^{15}\ \mathsf{G}}{B}\right)\left(\frac{n_e}{10^{-4}\ \mathsf{fm}^{-3}}\right) \times \left(\frac{L}{100\ \mathsf{cm}}\right)^2 \left(\frac{1}{|1 - 4\pi\chi_n \sin^2\theta_B|}\right)^{1/2}\ \mathsf{s},$$

  $L =$ characteristic length scale
- Can be viscously suppressed if crust undergoes plastic failure
- Also obtain unstable Alfvén modes $\omega \approx \omega_{\mathsf{A}}\sqrt{1 - 4\pi\chi_n \sin^2\theta_B} \to$: analog to core instability

- Temperature also suppresses instability by reducing $|\chi_n|$

T_{crit} for $\chi_n < 1/(4\pi)$ (K)

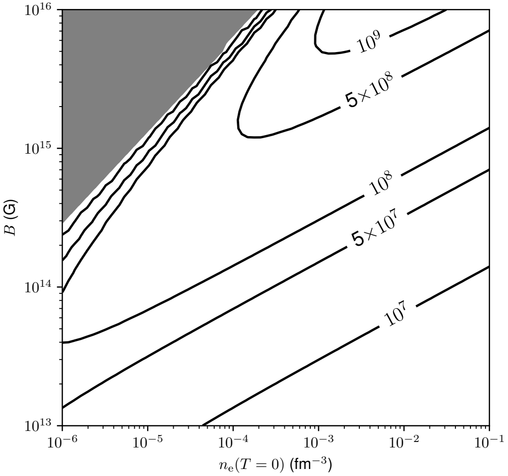

Shaded region is always stable

Magnetic domain formation

- $\eta = 1 - 4\pi\chi_n < 0$ indicates thermodynamic instability $\rightarrow$ formation of magnetic domains
- Domains consists of alternating regions of two different values of magnetization, with equilibrium properties determined using Maxwell construction.

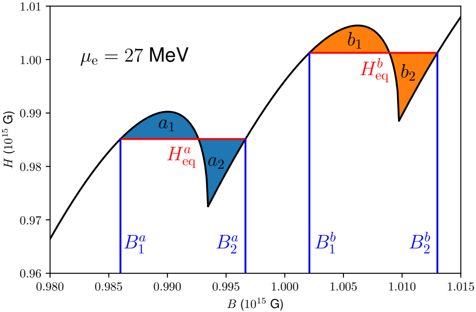

- Reduction in free energy associated with domain formation $\sim 10^{-6}$ of total energy density

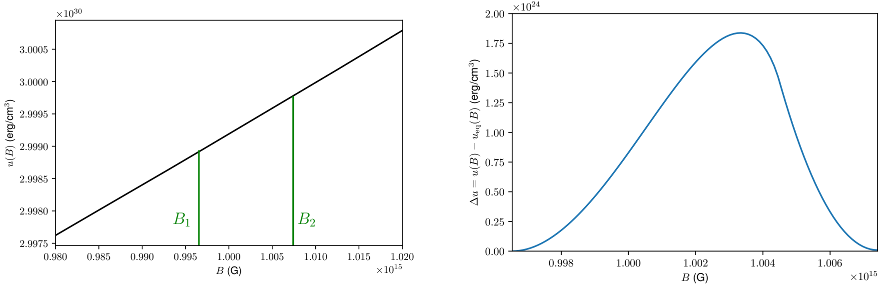

- Domains observed in the laboratory at cryogenic temperatures: Condon (1966), Pippard (1980), Shoenberg (1984), etc.
- Implications of such domains studied in neutron stars by Blandford and Hernquist (1982) and Suh and Mathews (2010), but they focused on the effects of magnetostrictive forces to "crack" the crust

Magnetar heating problem

- Magnetar surface luminosities are systematically higher than theoretically predicted without an additional heat source
- Strong magnetic field likely responsible for this heating (ambipolar diffusion in core, mechanical dissipation in magnetically-stressed crust, crustal Ohmic dissipation, bombardment of surface by charged particles) [Beloborodov and Li 2016]
- Reasons to disfavor these mechanisms outside of very specific conditions (e.g., $B \gtrsim 10^{16}$ G or B varying over short length scales)

- E.g., Potekhin and Chabrier (2018) included Landau quantization in crust transport (plus proton SC) $\rightarrow$ increased magnetar surface luminosity (i.e., surface temperature) at $t \sim 10^3$–10^4 years.
- *But* only sufficient to explain luminosity of $\sim$ half of known magnetars

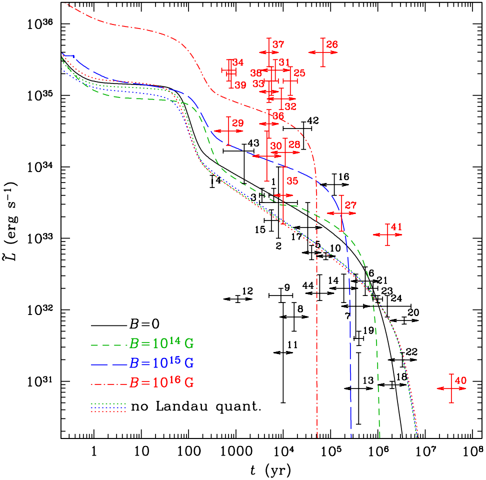

[Potekhin and Chabrier, A&A **609**, A74 (2018); red crosses are magnetars]

Domain formation-associated heating?

- Consider a scenario in which thermal evolution or field evolution causes a region of the crust to become unstable
- Timescale for domain formation $\sim \tau_{\mathrm{O}} = 4\pi\sigma L^2/c^2$ [Blandford and Hernquist 1982]: longer than timescale of strong-field Hall MHD, unstable crust Alfvén mode instabilities
- Unstable field growth over short length scales $\sim$ size of domain

- Generates field inhomogeneities that are fractionally small, but also of limited spatial extent $\sim$ size of domain $\sim$ spacing between domains $\Delta z \sim$ 100 cm
- Maximum energy density released per domain is $\Delta u \sim 10^{24}$ erg/cm^3
- For uniform $B = 10^{15}$ G, will have $N_{\text{inst}} \sim 100$ potentially unstable regions in crust

- Estimate heating rate per unit area due to Ohmic dissipation of unstable-grown fields

$$F_{\mathsf{O}} \approx N_{\mathsf{in}} \frac{\Delta u \Delta z}{\tau_{\mathsf{O}}} \approx 10^{21} \left(\frac{N_{\mathsf{in}}}{100}\right) \left(\frac{10^{24}\ \mathsf{s}}{\sigma}\right) \left(\frac{\Delta u}{10^{23}\ \frac{\mathsf{erg}}{\mathsf{cm}^3}}\right) \left(\frac{100\ \mathsf{cm}}{\Delta z}\right) \frac{\mathsf{erg}}{\mathsf{cm}^2\ \mathsf{s}},$$

- For magnetars to sustain their hot surface temperature, the crustal heating mechanism must provide a heat flux $F \sim 10^{24}$ erg cm^{-2} s^{-1} [Beloborodov and Li 2016], so this effect is too small
- *Very optimistic* if standard field evolution and cooling are only mechanisms responsible for destabilization

Enhanced Ohmic dissipation?

- Joule heating rate is roughly

$$\dot{q}_{\mathrm{O}} = \frac{1}{\sigma} J_e^2 = \frac{c^2}{16\pi^2\sigma} (\boldsymbol{\nabla} \times \boldsymbol{H})^2 \sim \frac{c^2}{16\pi^2\sigma} \eta^2 (\boldsymbol{\nabla} \times \boldsymbol{B})^2.$$

- dHvA oscillations of η could help amplify Joule heating if sufficiently large
- Since conductivities are lower in the crust, effect should be most significant here
- Could enhanced Ohmic dissipation help explain higher magnetar temperatures compared to other neutron stars?

Questions:

1. Are magnetization effects (more specifically, the differential magnetic susceptibility) significant enough to modify the global magneto-thermal evolution of magnetars?
2. When Landau quantization effects are included in both transport and thermodynamics, do their effects on magneto-thermal evolution enhance or cancel each other?
3. Interplay between effects of dHvA oscillations of η and thermal evolution?

In progress: Numerical simulations of magneto-thermal evolution with Landau quantization effects

- Solve:
    1. Magnetic induction equation with the Hall effect and Ohmic dissipation; current includes Landau quantized-derived differential magnetic susceptibility
    2. Heat equation with heat diffusion, Joule heating and neutrino emissivity (cooling)
- Can turn on/off Landau quantization effects in thermal and electrical conductivities, specific heat capacity, differential magnetic susceptibility. Include anisotropic conductivities.

Simulation details

- Uses `Dedalus v.3` [Burns, Vasil, Oishi, Lecoanet and Brown 2020], a PDE solver library for Python using spectral methods and symbolic equation entry
- Realistic neutron star crust density and composition profile from BSk24 EOS [Pearson et al. 2018]
- Assume core temperature follows Potekhin and Chabrier (2018) thermal evolution simulation, and $\boldsymbol{B}$ is expelled from core: want to avoid simulating core, concentrate resolution to resolve more SdH/dHvA oscillations

Magnetic field evolution at fixed T

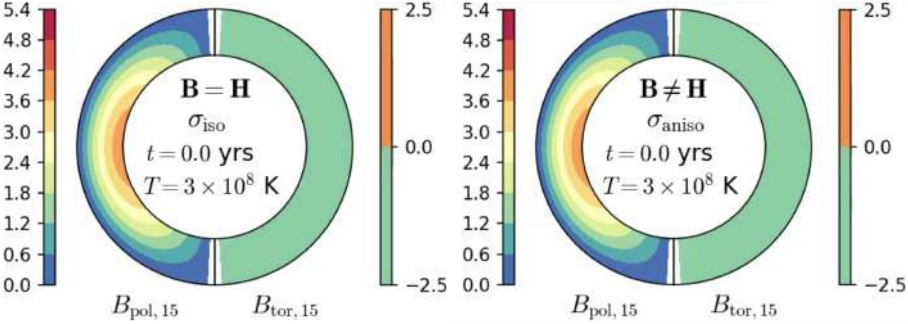

- Changes to field topology: more small-scale structure generated by Hall term with Landau quantization included

- Landau quantization in σ, $\eta = 1 - 4\pi\chi_n$ can both increase field energy dissipation, but latter more important. Effects not necessarily additive

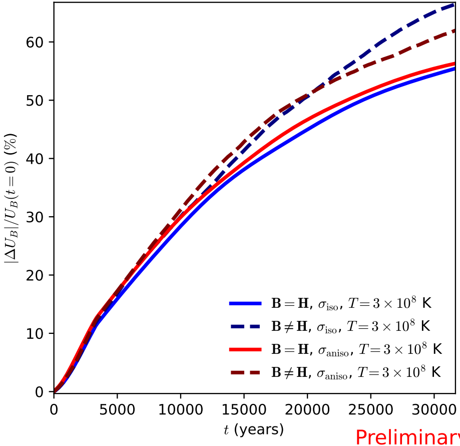

Preliminary

- Landau quantization in σ, $\eta = 1 - 4\pi\chi_n$ can both increase field energy dissipation, but latter more important. Effects not necessarily additive
- More pronounced effects with decreasing T

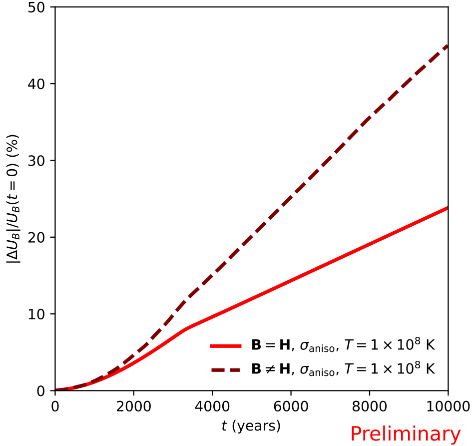

Magneto-thermal evolution

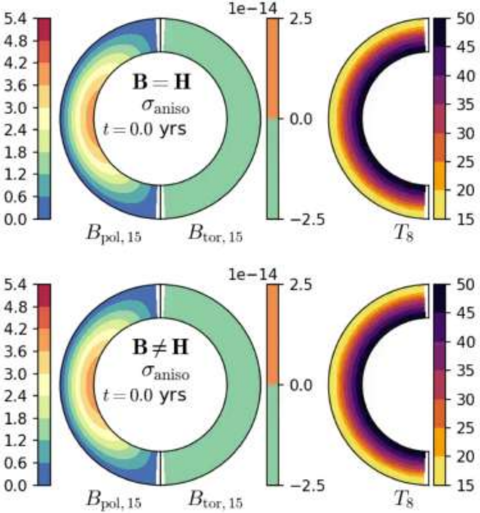

Conclusions

- We find MHD instabilities in the core and crust associated with Landau quantization of electrons at high densities and magnetic fields relevant to magnetars
- Instabilities are suppressed in equilibrium by formation of magnetic domains; system could be locally destabilized by B, T evolution
- Enhanced Ohmic dissipation due to dHvA oscillations of differential magnetic susceptibility occurs in crust for $T \lesssim 3 \times 10^8$ K ($t \gtrsim 10^3$ years) for $B \sim 10^{14}$–10^{15} G

Extra slides

Magnetic buoyancy

- $\boldsymbol{k} \parallel \boldsymbol{B}$ perturbations have associated magnetic buoyancy instability
- Simpler case: for $\boldsymbol{k} \perp \boldsymbol{B}$ case, the magnetic buoyancy stability criterion is

$$\frac{c_s^2 \tilde{N}^2(B)}{g} + \frac{B^2}{4\pi\rho}\eta\frac{\mathsf{d}}{\mathsf{d}r}\ln\left(\frac{B}{\rho}\right) + B\mathcal{M}_\rho\frac{\mathsf{d}\ln\rho}{\mathsf{d}r} > 0$$

where $\tilde{N}(B)$ = Brunt–Väisälä (buoyant) frequency including magnetic field-dependent terms.

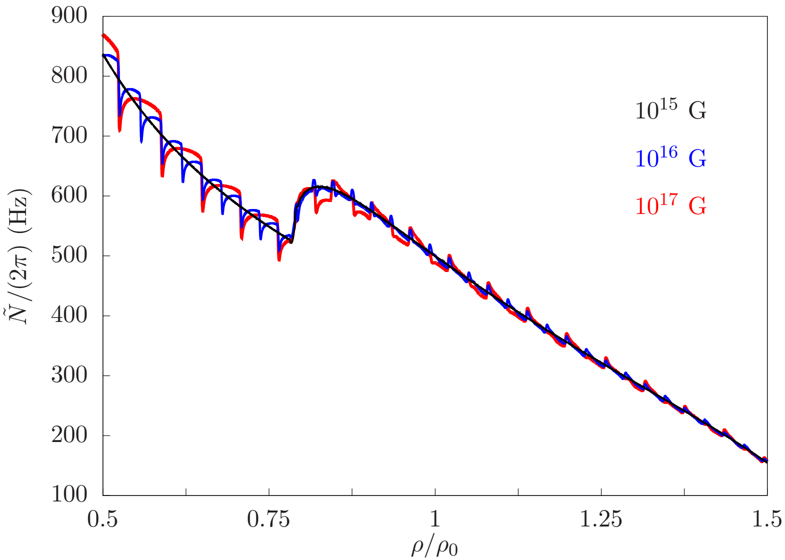

900
800
700
600
500
400
300
200
100
$\tilde{N}/(2\pi)$ (Hz)
0.5
0.75
1
1.25
1.5
ρ/ρ_0
10^{15} G
10^{16} G
10^{17} G

- In $\boldsymbol{k} \perp \boldsymbol{B}$ case, $\tilde{N}(B)$ is too large to allow magnetic buoyancy instability
- In $\boldsymbol{k} \parallel \boldsymbol{B}$ case, $\mathrm{d}\ln\left(\frac{B}{\rho}\right)/\mathrm{d}r \to \mathrm{d}\ln B/\mathrm{d}r$, which permits instability (instability criterion shown at right): these contributions are much smaller than other destabilizing terms except for longest wavelength perturbations $\lambda \sim R_\star$

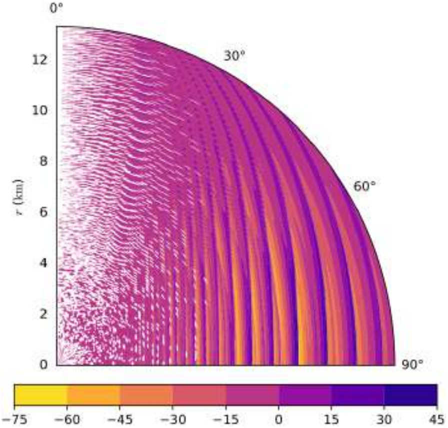

Magneto-thermal evolution simulation equations

$$\frac{\partial \boldsymbol{A}}{\partial t} = -c\boldsymbol{\nabla}\Phi - \frac{1}{n_e e}\boldsymbol{J}_e \times \boldsymbol{B} - c\left(\frac{\boldsymbol{J}_{e,\parallel}}{\sigma_\parallel} + \frac{\boldsymbol{J}_{e,\perp}}{\sigma_\perp}\right)$$

$$\boldsymbol{J}_e = \frac{c}{4\pi}\boldsymbol{\nabla} \times \boldsymbol{B} - c\left(\chi_n \boldsymbol{\nabla} B + \mathcal{M}_n \boldsymbol{\nabla} n_e\right) \times \hat{\boldsymbol{B}}$$

$$c_{V,B}\frac{\partial T}{\partial t} = -\boldsymbol{\nabla}\cdot\boldsymbol{q} + \frac{1}{\sigma_\parallel}\boldsymbol{J}_{e,\parallel}^2 + \frac{1}{\sigma_\perp}\boldsymbol{J}_{e,\perp}^2$$

$$-\dot{q}_\nu - T\left(\frac{s_\mathsf{e}}{n_\mathsf{e}} - \left.\frac{\partial s_\mathsf{e}}{\partial n_\mathsf{e}}\right|_{T,B}\right)(\boldsymbol{v}_\mathsf{e}\cdot\boldsymbol{\nabla})n_e$$

$$\boldsymbol{q} = -\kappa_\parallel \hat{\boldsymbol{B}}(\hat{\boldsymbol{B}}\cdot\boldsymbol{\nabla}T) + \kappa_\perp\left(\hat{\boldsymbol{B}}\hat{\boldsymbol{B}} - \boldsymbol{I}\right)\cdot\boldsymbol{\nabla}T,$$